

Vibrational and rotational population distribution of D_2 associatively desorbing from Pd(100)

D. Wetzig, M. Rutkowski, and H. Zacharias

Physikalisches Institut, Westfälische Wilhelms-Universität Münster, Wilhelm-Klemm-Straße 10, 48149 Münster, Germany

A. Groß

Physik Department T30, Technische Universität München, D-85747 Garching, Germany

(Received 8 December 2000; published 30 April 2001)

The rotational and vibrational state distribution of D_2 molecules desorbing from Pd(100) is determined by tunable vacuum ultraviolet laser ionization spectroscopy. For the deuterium supply a permeation source is used operating at surface temperatures in the range from 400 to 850 K. The molecules are detected in rovibrational states up to $(v'', J'') = (0, 12)$ and $(1, 8)$. A significant rotational cooling is observed together with a strong vibrational heating. These experimental results are found to be in good agreement with quantum-mechanical calculations based on an *ab initio* potential-energy surface. A consistent microscopic picture of the hydrogen reaction dynamics on Pd(100) is established and thus a recent controversy about the application of the principle of detailed balance in the system D_2 /Pd(100) can be settled.

DOI: 10.1103/PhysRevB.63.205412

PACS number(s): 68.03.Fg, 82.20.Kh, 68.49.Uv

I. INTRODUCTION

The recombination of two hydrogen atoms on a metal surface represents the simplest but most fundamental catalytic surface reaction. This molecular desorption phenomenon was investigated extensively in the past, with particular attention devoted to all molecular degrees of freedom: rotational and vibrational energy, internal state specific velocity and angular distributions, and the influence of the alignment of the rotational angular momentum for various substrates. Overviews of the experimental and theoretical investigations are given by a number of review articles,^{1–3} respectively. The theoretical investigations are based on the density-functional theory (DFT). The six-dimensional potential-energy surface (PES) which describes all hydrogen molecular degrees of freedom and the various positions within the surface unit cell has been calculated by several groups for the benchmark systems H_2 /Pd (Refs. 4–7) and H_2 /Cu (Refs. 8–10) and further substrates.^{6,11} In all cases the PES is both energetically and geometrically corrugated which means that the height as well as the location of the dissociation barrier varies within the surface unit cell. On six-dimensional potential-energy surfaces quantum dynamical calculations of the sticking probability of hydrogen have been performed for H_2 /Pd(100),^{12–15} H_2 /(2×2)S/Pd(100),^{16,17} H_2 /Cu(100),^{18,19} and H_2 /Cu(111).^{20,21} In these simulations all six hydrogen degrees of freedom were explicitly taken into account while the substrate was kept fixed. Since the dynamical calculations were performed within the Born-Oppenheimer-approximation, the influence of electron-hole pairs were neglected. In the only DFT-based study that considers also the motion of the substrate atoms of the surface two hydrogen molecular degrees of freedom and one palladium surface vibrational mode were included in simulations of the subsurface absorption of H_2 /Pd(111).²²

Experimentally a large number of studies have been performed that focused either on the hydrogen dissociative adsorption on metal surfaces^{23–25} or the recombinative desorption from these surfaces.^{26–29} Note that adsorption and

desorption are related through time-reversal symmetry. The initial dissociative sticking probability of H_2 on various Cu surfaces has been measured by molecular beam techniques.^{30–33} The results indicate a dissociation barrier which is accessed through energy partition in both translational and vibrational degrees of freedom in the impinging hydrogen molecule. Michelsen *et al.*³⁴ have found that D_2 desorption measurements made over a range of Cu(111) surface temperatures cannot be adequately accounted for by a single function of the sticking probability on the incidence energy and angle. It is found necessary to allow this function to vary slightly with surface temperature caused by the motion of surface atoms. Rettner *et al.* have investigated the dependence of the translational energy of $H_2(v, J)$ on the rotational and vibrational states formed in recombinative desorption from Cu(111).³⁵ The mean kinetic energy determined from time-of-flight (TOF) measurements depends strongly on both rotational and vibrational states. Rotational motion is found to hinder adsorption for low rotational states ($J < 4$) and enhance adsorption for high rotational states. But the rotational energy is less effective than the vibrational energy in promoting adsorption. The sticking probability of H_2 /Pd(100) was determined by molecular beam experiments.²³ Furthermore, Watt and Sitz performed scattering experiments of H_2 /Pd(111) as a function of surface temperature.³⁶ The rotational excitation in scattering was found to depend on the surface temperature, in particular for excitation energies larger than the incident kinetic energy, i.e., when the incident energy was not sufficient to supply enough excitation energy and thus energy transfer from the surface to the molecule was necessary.

In our experimental group we have previously investigated the velocity distribution of H_2 and D_2 molecules desorbed from the clean Pd(100) surface at various temperatures between 440 and 770 K.³⁷ The velocity distributions are found to be Maxwell-Boltzmann-like. The kinetic energy of hydrogen molecules agrees with that expected for molecules in thermal equilibrium with the surface, while for deuterium molecules the average kinetic energy is about 10–30 meV

higher than expected in a thermal equilibrium. The rotational population distribution of different internal states of H_2 and D_2 desorbing from Pd(100) has been previously investigated by Schröter *et al.*³⁸ for low rotational states up to $J''=5$ in the vibrational ground state. A significant rotational cooling effect has been observed which leads to rotational temperatures of about 350 K for all investigated surface temperatures between 325 and 740 K. Also the amount of vibrationally excited D_2 molecules in desorption has been measured.³⁹ The population in the state $v''=1$ increased exponentially with the surface temperature T_S , associated with an activation energy that is less than the activation energy of free D_2 molecules.

Improvements in the experimental detection techniques enable now the detection of deuterium molecules up to $J''=12$ in the vibrational ground state and up to $J''=8$ in the first vibrational excited state. Thus we can measure the behavior of the rotational state distribution over a wide range of rotational energies. The population of vibrational excited states are determined and compared with the expected state population of the desorbing molecules in the thermal equilibrium. The inclusion of higher rotational states modifies the experimental results for the rotational and vibrational temperature in $\text{D}_2/\text{Pd}(100)$ desorption with respect to previous findings^{38,39} and leads to a reinterpretation of these results. We still find rotational cooling and vibrational heating in desorption, but the deviations from thermal equilibrium are somehow less than derived in previous studies.

We have compared the experimental results with quantum-mechanical calculations of the hydrogen dissociation based on an *ab initio* potential-energy surface. The agreement between experiment and theory is very satisfying. Thus a consistent microscopic picture of the dynamics of the hydrogen interaction with Pd(100) is provided. In addition, a recent controversy about the application of the principle of detailed balance in the system $\text{D}_2/\text{Pd}(100)$ (Ref. 40) can be settled.

This paper is structured as follows. After this Introduction we briefly recall the main technical details as far as experiment and theory are concerned. Then we present the results of the rotational and vibrational distribution in desorption and finally discuss these findings in the context of the calculations.

II. TECHNICAL DETAILS

A. Experimental method

The experimental setup has been described in detail in an earlier publication.³⁸ The experiments are carried out in an UHV chamber evacuated by a turbomolecular and a cryo pump to a base pressure of less than 1×10^{-10} mbar. Low-energy electron diffraction (LEED) and retarding field Auger-electron spectroscopy is used to check the order and cleanliness of the sample surface. Argon-ion sputtering at low energy (0.5 keV) is employed to clean the surface before each measurement. After sputtering the surface is allowed to anneal before an experimental run. The hydrogen desorption flux is provided by permeation through a sealed single-crystal palladium disk, which is soldered with gold by rf

heating in high vacuum to a high-purity (99.99%) Ni support cylinder.⁴¹ Near the crystal this nickel cylinder has comparatively thick walls (5.5 mm) to suppress hydrogen permeation through nickel. This permeation source is radiatively heated by a concentric oven to temperatures between 400 and 850 K. The whole assembly is mounted on a five-axis manipulator. The D_2 stagnation pressure is adjusted in the 10 to 500 mbar range, dependent upon the crystal temperature, in order to keep about the same desorption flux at all temperatures. During desorption the average pressure in the chamber thus rises to about 1×10^{-7} mbar. The measured desorption flux is in good agreement with the one calculated from literature data about the permeation energy of D_2 in palladium.⁴²

Rovibrational population distributions of desorbing deuterium molecules are measured by resonantly enhanced two-photon ionization (REMPI). The REMPI detection region is separated from the desorption chamber by a copper plate with a central aperture of 10-mm diameter. The state selectivity is achieved with tunable vacuum ultraviolet (VUV) laser radiation by single-photon excitation of the $B^1\Sigma_u^+ \leftarrow X^1\Sigma_g^+$ Lyman transitions around $\lambda=106\text{--}110$ nm. This tunable VUV light is generated by frequency mixing the output of a frequency-doubled pulsed dye laser in krypton and xenon.⁴³ The conversion efficiency in the frequency-tripling process is typically about 10^{-5} to 10^{-6} . The VUV radiation generated in the rare-gas cell is recollimated with a LiF lens. Including the absorption loss in the LiF lens, which separates the conversion cell from the UHV chamber, a pulse energy of about 10 nJ of tunable VUV radiation is available in the interaction region with the desorption flux. The intensity of the VUV beam is continuously monitored at the exit of the desorption chamber with an ionization cell filled with acetone. The deuterium-ion signal is normalized to the pulse energy of the VUV laser. Within the tuning range of krypton it is possible to excite rotational lines of the (0–0) to (3–0), and (3–1) to (5–1) Lyman bands of D_2 .

After the excitation to the B state the electronically excited molecules are ionized by a second UV laser photon ($\lambda=266$ nm) which is derived by frequency quadrupling from the output of the fundamental Nd:YAG (where YAG means yttrium aluminum garnet) laser. The pulse energy of the ionizing laser is kept constant at 2.5 mJ and monitored by a photodiode behind the main chamber. Both the exciting VUV and the ionizing UV laser beams overlap at a distance of 20 mm in front of the Pd surface and cross each other at an angle of 14° in a plane parallel to the surface. The UV and VUV radiation are both polarized parallel to the surface normal. Deuterium ions are detected by a two-stage micro-channel plate (MCP) assembly with a 50- Ω impedance-matched anode mounted at a right angle to the desorption flux. The output of the MCP detector is processed by an integrating electronic and simultaneously transferred to a microprocessor.

In REMPI detection of hydrogen and its isotopes the deduction of rotational state populations from the measured ion signal poses a special problem. Due to dominant autoionization the ionization cross section of the $B^1\Sigma_u^+$ state—as well as other intermediate states such as e.g., the $E, F^1\Sigma_g^+$

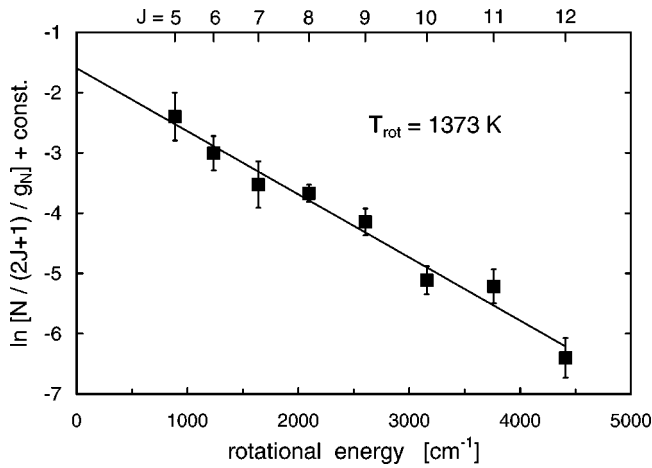


FIG. 1. Boltzmann plot of the rotational state distribution of D_2 from a Knudsen cell at $T=1360$ K. The molecules are detected by LIF. The fit (solid line) to the data yields a rotational temperature of $T_{rot}=(1373\pm 15$ K).

states—depends strongly upon the ionization wavelength and the specific rovibrational states.^{44,45} By comparing, however, the line heights in a spectrum of known population distribution to those being investigated relative ionization probabilities can be derived, and thus the population of rotational levels in the desorption flux can be obtained. Such a known rotational state population distribution can either be provided by back-filling the chamber with hydrogen at room temperature or from the flux out of a hot Knudsen cell. We employed both methods since at room temperature only low J'' states of D_2 are sufficiently populated. A cylindrical Knudsen cell with an aperture of $80\text{-}\mu\text{m}$ diameter is radiatively heated up to 1500 K. The temperature of the cell is measured by a pyrometer and a Pt/Pt-Rh thermocouple. High-purity deuterium gas generated by resistively heating a palladium leak is supplied to the Knudsen cell. At a pressure of 0.15 mbar a measured flux of $q_{pV}=4\times 10^{-4}$ mbar l s^{-1} through the cell corresponds to the molecular flux expected through an aperture with the diameter of $80\text{ }\mu\text{m}$. The deuterium flux can be adjusted by the temperature of the Pd leak and the backing pressure of the D_2 . In a first step the population distributions in the back-filled chamber and the flux from the Knudsen cell are determined by laser-induced fluorescence (LIF), because for this detection scheme the transition probabilities are known. In all cases Boltzmann distributions of the rotational state populations are found that correspond to the respective temperatures of the chamber and the Knudsen cell.

Figure 1 shows in a Boltzmann plot the population distribution in a flux from a Knudsen cell held at $T=1360$ K. The populations in the vibrational ground state are determined from the fluorescence signals and the known excitation probabilities (the Hönl-London factor, the Franck-Condon factor). Since the rotational states are probed via different vibronic bands of the $B^1\Sigma\leftarrow X^1\Sigma$ transition, also the relative quantum efficiency of the solar blind photomultiplier (EMR 541-G-08-18) and the transmission through a MgF_2 window have to be accounted for. From the slope of a linear regression to the data a rotational temperature of 1373 K is derived, in good agreement with the temperature of the Knud-

sen cell. After this confirmation of the expected rotational state population distribution of molecules in the flux from the Knudsen cell the relative ionization probabilities for each rovibrational state probed at the given laser intensities are determined for (VUV+UV) REMPI. In this way relative ionization probabilities are obtained for $X^1\Sigma_g^+$ ($v''=0$, $J''=6$ to 12) and ($v''=1$, $J''=0$ to 8). For ($v''=0$, $J''=0$ to 6) we derived the ionization probabilities from a gas-phase ensemble at a chamber temperature of 300 K.

Since the experiments are carried out with a continuous desorption flux, some molecules can reach the detection volume after having thermally equilibrated at the chamber walls. Such molecules give rise to a background that has to be accounted for in the analysis of rotational lines from $J''=0$ to 6 of the vibrational ground state. In higher rotational states and in ($v''=1$) no significant population is found at room temperature. We measured this background separately by removing the Pd crystal about 10 cm from the detection plane and rotating it by 90° while keeping the desorption flux constant. In this way only molecules that have equilibrated on the walls are measured.

B. Theory

The theoretical background of the calculations has been described in detail in Ref. 13. Here we only recall some fundamentals. The interaction potential of hydrogen with the Pd(100) surface has been determined by density-functional theory (DFT) calculations in the generalized gradient approximation.⁴ These *ab initio* results have been parameterized by an analytical expression to yield a continuous potential-energy surface (PES).¹³ This PES has been used in quantum-mechanical coupled-channel calculations,⁴⁶ in which all six hydrogen degrees of freedom were explicitly taken into account; the substrate, however, was kept fixed. This is a reasonable approximation considering the large mass mismatch between hydrogen and palladium.

In the quantum-mechanical simulations state-specific sticking probabilities $S_n(E_\perp)$ as a function of the incident normal kinetic energy E_\perp are determined. Here n stands for a multi index that describes the initial vibrational, rotational, and parallel momentum states of the molecule. From these sticking probabilities vibrational and rotational distributions in desorption are derived via the principle of detailed balance or microscopic reversibility.⁴⁰ In detail, the population D_n of the state n in desorption at a surface temperature of T_s is given by

$$D_n(E_\perp) = \frac{1}{Z} S_n(E_\perp) e^{-(E_n + E_\perp)/k_B T_s}. \quad (1)$$

Here E_\perp is the kinetic energy perpendicular to the surface, E_n is the energy associated with the internal state n , and Z is the partition sum that ensures the normalization of the distribution. To obtain the mean vibrational and rotational energies in desorption, the appropriate average over the probabilities D_n has to be performed. Since the substrate is kept fixed in the simulation, it does not participate dynamically in the adsorption/desorption process. Still it is assumed

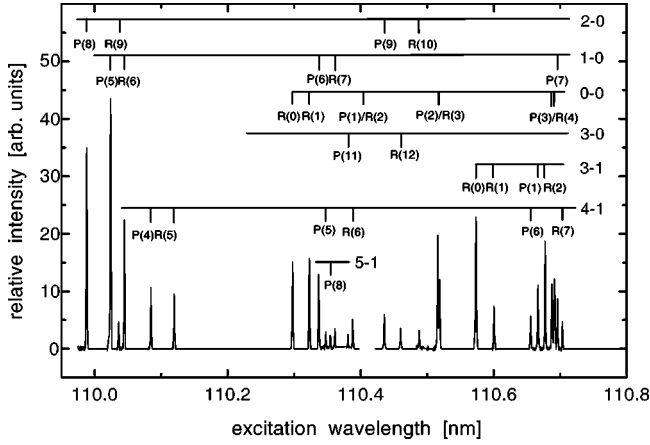


FIG. 2. Resonantly enhanced VUV laser ionization spectrum of deuterium desorbing from Pd(100), $T_s=800$ K.

to act as a heat bath that determines the population distribution of the molecular states in desorption.

III. RESULTS AND DISCUSSION

A. Rotational population

In Fig. 2 a typical $(1+1')$ REMPI spectrum from 109.9 to 110.8 nm of D_2 desorbing at a temperature $T=800$ K from a clean Pd(100) surface is shown. The signal is normalized to the intensity of the exciting VUV laser radiation. The intensity of the ionizing laser at 266 nm is constant during the measurement. A line identification is given at the top of the spectrum. Besides rotational lines of $(0-0)$ to $(3-0)$ Lyman bands also lines of vibrationally excited molecules in the $(3-1)$, $(4-1)$, and $(5-1)$ bands are clearly resolved and identified. Rotational state populations of $J''=0$ to 12 in the vibrational ground state and $J''=0$ to 8 in the first excited vibrational state have been measured. In this experiment the polarization of the exciting VUV and the ionizing UV laser beams are parallel to each other and parallel to the surface normal. From spectra like that shown in Fig. 2 the population $N(v''=0, J'')$ and $N(v''=1, J'')$ of the rotational levels in the vibrational ground state and in the first excited state can be obtained. As mentioned earlier, the relative ionization probability of each initial rovibrational state needs to be considered.

For the derivation of the state population the integral of the ionization lines is considered. The relative population $N(v'', J'')$ of the rovibrational initial state can be determined from this integral I by

$$N(v'', J'') \propto I / [|R_e^{n'n''}|^2 |R_{vib}^{v''v''}|^2 S_{J', J''} K(v', J') \chi]. \quad (2)$$

Here $|R_e^{n'n''}|^2$ and $|R_{vib}^{v''v''}|^2$ denote the electronic transition moment and the Franck-Condon factor, respectively, and $S_{J', J''}$ describes the Hönl-London factor. $K(v', J')$ takes the relative detection sensitivity as determined in Sec. II into account. The influence of the rotational alignment of desorbing molecules is described by the polarization factor χ . This factor χ compensates for aligned molecules the dependence

TABLE I. The polarization factor χ compensates the dependence of the excitation probability on the angle between the polarization of the exciting laser and the transition moment of the molecule.

J	1	2	3	4	5	6	7	8
P branch	1	1	1.03	1.16	1.34	1.21	1.08	1.03
R branch	1	1	1.01	1.07	1.16	1.12	1.05	1.02

of the excitation probability on the angle between the transition moment and the polarization of the exciting laser.

In order to derive state populations the intensity $I=(I_{\parallel}+I_{\perp})/2$ has to be known. Here I_{\parallel} and I_{\perp} denote ion intensities for the polarization of the exciting laser being parallel and perpendicular to the surface normal \hat{n} , respectively. In the present experiment ion intensities I_{\parallel} are measured. I_{\perp} can be related to I_{\parallel} by

$$I_{\perp} = I_{\parallel} \frac{1-P}{1+P}, \quad (3)$$

where P denotes the anisotropy. P can be obtained from the quadrupole alignment factor $A_0^{(2)}$ which has been determined in an earlier experiment.⁴⁷ The correction factor χ is thus given by

$$\chi = \frac{1}{1+P}. \quad (4)$$

The alignment of the molecules affects the intensity measurements for the same J'' via the P and R branch differently, because the connection between the quadrupole alignment factor $A_0^{(2)}$ and the anisotropy P depends also on the transition.⁴⁸ The appropriate values for the anisotropy factors P for different rotational states as derived from measured alignment values $A_0^{(2)}$ ⁴⁷ are listed in Table I. For rotational states larger than $J''=8$ experimental data for the alignment are not available; we thus set $\chi=1$ for these states. In the vibrationally excited state no rotational alignment was observed within the experimental error.⁴⁷

Rotational state populations for D_2 desorbing from a clean Pd(100) surface at $T=800$ K are shown in Fig. 3 for both vibrational states $v''=0$ and $v''=1$, indicated by filled squares and triangles, respectively. The population data displayed in Fig. 3 are averaged for the P - and R -branch measurements. The ortho- and para- D_2 fit to common curves, implying that they are populated statistically. For an ensemble in thermal equilibrium a Boltzmann plot as shown in Fig. 3 should exhibit a linear dependence with a slope of $(-1/k_B T_{rot})$. As is evident, the rotational state population data of the vibrational ground state do not resemble a Boltzmann distribution, although the deviation from a Boltzmann distribution seems to be small. But to illustrate it more clearly a Boltzmann fit to the population data of the states $J''=5$ to 12 is shown as a thin line yielding a rotational temperature of $T_{rot}=906$ K. The overpopulation of low rotational states $J''=0$ to 4 can thus clearly be indicated. It is possible to fit the population distribution by two Boltzmann

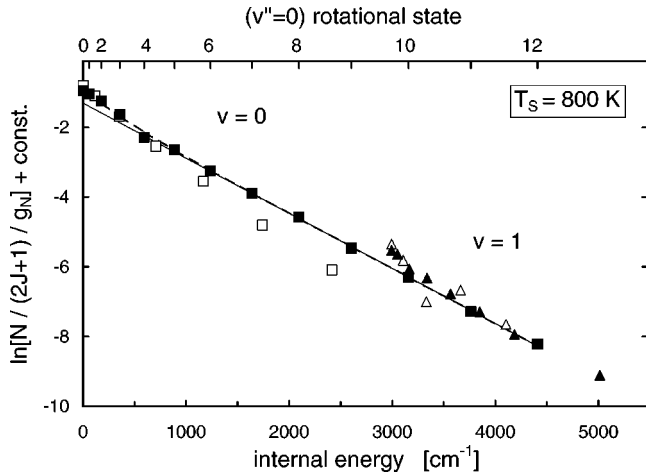


FIG. 3. Boltzmann plot of the rotational population distribution of D_2 desorbing from Pd(100) at $T_S=800$ K. Filled squares denote molecules in ($v''=0$) and triangles in ($v''=1$). Also theoretical values for H_2 molecules in the states $v''=0$ and $v''=1$, respectively, are shown (open symbols).

temperatures of $T_1=352$ K and $T_2=910$ K, as shown by the dashed curve in Fig. 3. This composed fit thus reveals a strong rotational cooling effect for D_2 in low- J'' states, while the higher J'' are more or less in thermal equilibrium with the surface. Similar distributions are observed at all surface temperatures investigated. Fits to the data of the rotational states $J''=5$ to 12 yield rotational temperatures higher than the corresponding surface temperature, $T_{rot} > T_S$. This can be rationalized by the following model. As mentioned, molecules in low- J'' states, $J'' \leq 3$ or 4, can effectively be steered to an unactivated adsorption position within the surface unit cell. Similarly, molecules in high- J'' states have sufficient rotational energy to overcome after rotational-translational coupling any barrier in the dissociative adsorption potential on Pd(100). Thus their sticking probability is high. Molecules in $J''=5$, however, cannot be effectively steered nor do they have sufficient energy to overcome the barrier. Thus their sticking probability is lower and a significant fraction is reflected. The observation that T_{rot} appears to be higher than T_S for $J''=5$ to 12 is due to the fact that the $J''=5$ is lower than thermal equilibrium when detailed balance arguments are involved.

To account for the non-Boltzmann behavior of the rotational distribution the rotational energy $\langle E_{rot} \rangle = \sum_{J''} N(v'', J'') E_{rot}(J'')$ is used. For desorption in the vibrational ground state $v''=0$ at $T_S=800$ K, as displayed in Fig. 3, we obtain $\langle E_{rot} \rangle = 528 \text{ cm}^{-1}$ or $\langle E_{rot} \rangle / k_B = 761$ K. For molecules desorbing in $v''=1$ the corresponding rotational energy amounts to $\langle E_{rot} \rangle = 519 \text{ cm}^{-1}$ or $\langle E_{rot} \rangle / k_B = 747$ K.

The stronger rotational cooling for hydrogen desorbing from clean Pd(100) reported earlier³⁸ was caused by a restriction to rotational states $J \leq 5$ due to insufficient sensitivity to detect higher J'' states. In addition, this result was influenced by the fact that the rotational alignment of the desorbing molecules was not known, which influences mainly low- J'' states for H_2 /Pd.

The experimental data are successfully simulated by

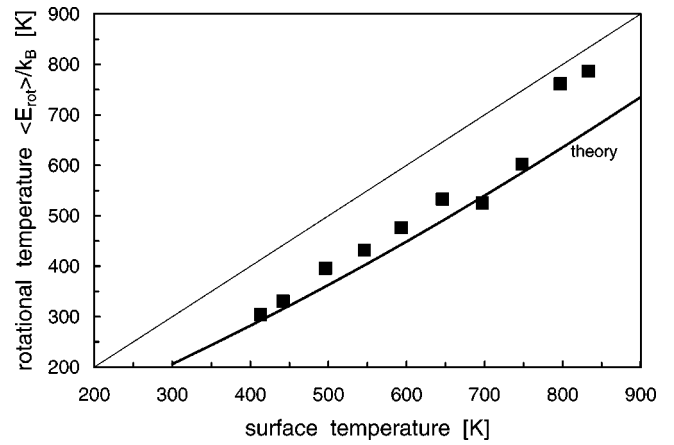


FIG. 4. Rotational temperature of D_2 desorbing at various surface temperatures from Pd(100) as a function of surface temperature (filled squares). The thin straight line denotes the line of thermal accommodation; the thick line represents the theoretical calculations for the desorption of H_2 /Pd(100).

quantum dynamic calculations performed on a six-dimensional potential-energy surface⁴ for H_2 /Pd(100). These calculations yield rotational state populations for H_2 molecules desorbing in both $v''=0$ and $v''=1$ vibrational states.¹² These data are included in Fig. 3 and indicated for by open squares and triangles for $v''=0$ and $v''=1$, respectively. These theoretical results show also a non-Boltzmann behavior of the rotational population.

The comparison between experiment and theory should be done with caution. The calculations are done for hydrogen while the experiments were performed with deuterium. Six-dimensional quantum-mechanical calculations are only feasible for the lighter hydrogen isotope. Due to the smaller mass significantly less channels have to be taken into account which decreases the computational effort tremendously. As far as the experiment is concerned, there are some studies of the hydrogen/Pd(100) system that have not found any significant isotope effect within the experimental uncertainties.²⁶ However, the kinetic energy³⁷ and the rotational alignment in hydrogen desorption from Pd(100) (Ref. 49) show a small isotope effect. For H_2 /Pd(111) also an isotope effect has been observed in molecular beam experiments.⁵⁰ These isotope effects are usually not dramatic and have only a small quantitative influence on the results. Theoretically only a small quantitative isotope effect has been found in lower-dimensional simulations.¹³ Hence it is reasonable to compare the experimental results for D_2 with the calculations for H_2 in a semiquantitative sense.

Rotational energies divided by k_B are shown in Fig. 4 for D_2 desorbing in $v''=0$ from clean Pd(100) as a function of surface temperature. The thin straight line in Fig. 4 indicates the expected behavior for complete accommodation of the rotational degree of freedom to the surface temperature. It is evident that the rotation is not in thermal equilibrium with T_S . For T_S up to about 750 K $\langle E_{rot} \rangle / k_B$ is lower than T_S by about 100 K. Mean rotational energies $\langle E_{rot} \rangle / k_B$ of H_2 in desorption calculated from the theoretical population data are also shown in Fig. 4 (thick line). A significant rotational

cooling is also obtained from these theoretical calculations. The agreement between experimental data and theoretical calculations is generally very good, within the experimental error. The remaining differences between experimental and theoretical values may be caused by an isotope effect.

Interestingly, in hydrogen adsorption on Pd(111) it was found that the rotational effects are stronger for H_2 than for D_2 .⁵⁰ This corresponds to our results plotted in Fig. 4 where the calculated rotational cooling is slightly stronger for H_2 than the measured one for D_2 .

One further source for deviations between experiment and theory is the assumption of a static substrate in the calculations. For the case of hydrogen subsurface absorption at Pd(111) Olsen *et al.*²² have found an influence of the surface motion on the energetic barriers. However, for adsorption on the surface the influence of the substrate motion should be smaller. On the other hand, in H_2 /Pd(111) scattering a large energy transfer between molecule and substrate was observed^{25,36} indicating that the substrate atoms do play a role in the interaction.

As far as the mechanism responsible for the rotational cooling is concerned, it is the same that is also responsible for the rotational hindering in adsorption via the principle of microscopic reversibility.⁵¹ The six-dimensional potential-energy surface for H_2 /Pd(100) shows a large corrugation and a strong anisotropy with respect to the barrier for dissociation. Molecules aligned spatially parallel to the surface can dissociate spontaneously, while for a perpendicular alignment an energetic barrier has to be surmounted.⁴ Molecules in low rotational states are steered more easily into a favorable orientation by the potential energy surface than molecules in highly rotating states. Thus molecules in such states are overpopulated in the desorption flux compared to the thermal equilibrium with the surface.

This rotational hindering in adsorption has indeed been observed in dissociative hydrogen reactions. Beutl *et al.*⁵⁰ measured the sticking probability of H_2 /Pd(111). Through seeding techniques they changed the kinetic energy of the molecular beam independently from the rotational energy of the impinging molecules. They showed that at low kinetic energies where the steering effect is most efficient an increase of the rotational energy of the incoming molecules at constant translational energy causes a drastic reduction of the sticking probability. Thus they confirmed the rotational hindering.⁵⁰ Later they refined their experimental techniques by using para- and *n*-hydrogen in the sticking of H_2 /Pt(110).⁵² Thereby they could determine state-resolved sticking probabilities. Also these experiments showed a pronounced decrease of the sticking probability with increasing rotational energy.

Using seeded molecular beams and rotationally state-selective laser detection, Gostein and Sitz obtained thus state-specific information for the scattering of H_2 /Pd(111).²⁵ They observed a strong dependence of the sticking coefficient on the rotational states $J''=0$ to 5. They found that the sticking coefficient first decreases as J'' is raised from 0 to 3. In fact it then increases again for $J''=4$ and 5. This eventual increase can actually be understood by a rotational to translational energy transfer⁵³ and has also been found in the

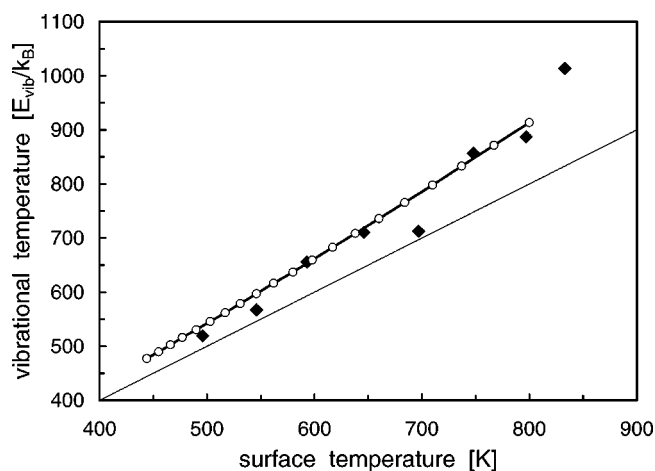


FIG. 5. Vibrational temperatures of D_2 desorbing at various surface temperatures from Pd(100) (filled diamonds). The straight line denotes again the thermal accommodation. The theoretical results are given by the open circles.

H_2 /Cu system.³⁵ These examples show that adsorption and desorption experiments and calculations¹⁵ provide a consistent picture of the rotational effects in hydrogen dissociation on metal surfaces.

B. Vibrational population

The vibrational temperature is determined from the relative population in the two vibrational states investigated. Figure 5 shows the measured vibrational temperatures for all surface temperatures studied as filled diamonds. The thin solid line represents again the line of full accommodation of the vibrational degree of freedom to the surface temperature. All experimental data show a temperature higher than the corresponding surface temperature. Obviously, an enhanced vibrational excitation occurs for recombinative D_2 desorption from a clean Pd(100) surface. The population of the $v''=1$ state is on average a factor of 1.76 higher than the corresponding thermal population. The theoretical values for the vibrational population obtained from the quantum dynamic calculations on the six-dimensional energy surface of the system H_2 /Pd(100) are shown by the open circles. Obviously, theoretical and experimental data again agree very well. The average vibrational overpopulation is calculated to be about a factor of 1.96 higher than the thermal equilibrium. Also this value agrees well with the experimental observation of a factor of 1.76.

We now discuss this overpopulation of the vibrational excited molecules in the desorption of hydrogen from the Pd(100) surface in comparison to the measured sticking probability in the same system.²³ In this molecular beam experiment the sticking coefficient has been determined as a function of the kinetic energy at a surface temperature of $T_S=170$ K. A sticking coefficient of 0.3 to 0.7 for kinetic energies of 0 to 400 meV was determined for H_2 . At a kinetic energy of 100 meV which corresponds to the kinetic energy of the desorbing molecules in the present desorption experiment³⁷ a sticking probability of about $S=0.35$ was ob-

tained. Using the principle of detailed balance, the vibrational population in desorption could thus be enhanced at most by a factor of $1/0.35=2.85$ if a sticking probability of unity is assumed for hydrogen molecules in the first excited vibrational state.

In an earlier publication we reported for D_2 desorbing in ($v''=1$) at $T_S=677$ K that the vibrational population is about nine times higher than expected for thermally equilibrated molecules.³⁹ This result was later questioned invoking detailed balance arguments as given above.⁴⁰ Indeed, a reanalysis of the previous results shows that the difference to the present study is caused by the fact that earlier the line heights of only two rotational lines with different J'' in $v''=0$ and 1 were compared under the assumption of the same population distribution in both vibrational states.³⁹ Presently, we determined the vibrational population by measuring many (v'', J'') lines and integrating over J'' , thus according to a good approximation for the whole vibrational population. Our new results are now in good agreement with the calculated overpopulation factors.⁴⁰ This resolves the controversy and demonstrates the applicability of the principle of detailed balance for the hydrogen interaction with metal surfaces. It should be noted that also the measured mean kinetic energies in hydrogen desorption from Pd(100) (Ref. 37) are in good agreement with the calculations.⁵⁴

An analysis of the calculations can be used in order to explain the source of the vibrational effects in hydrogen dissociation on Pd(100). They are not a consequence of the curvature of the relevant reaction path as in the strongly activated system H_2/Cu .^{3,53} They are rather caused adiabatically by the lowering of the hydrogen vibrational frequency upon dissociation.⁴⁰ This lowering has a stronger effect on the effective potential of the higher vibrational states, leading to the vibrational heating. This effect should be stronger for H_2 than for D_2 because of the higher vibrational frequency of H_2 which also leads to a larger absolute *change* in the frequency. In fact, the calculated vibrational heating for H_2 is on the average slightly larger than the measured one for D_2 . Thus the isotope effect provides an explanation for this deviation.

The vibrational heating is also shown in an Arrhenius analysis of the data in Fig. 6, where the logarithm of the vibrational population is plotted versus the inverse surface temperature. From a least-square fit of the measured data an activation energy of 402 meV is derived (straight line in Fig. 6). However, at $T_S \rightarrow \infty$, i.e., at $1/T_S \rightarrow 0$, all states are equally populated so that the ratio $N(v''=1)/N(v''=0)$ approaches unity. If one includes this value in the fit, an activation energy of 344 meV for the excitation of $D_2(v''=1)$ follows (dashed line in Fig. 6). The free D_2 molecule shows an excitation energy for $v''=1$ of 371 meV. At the clean

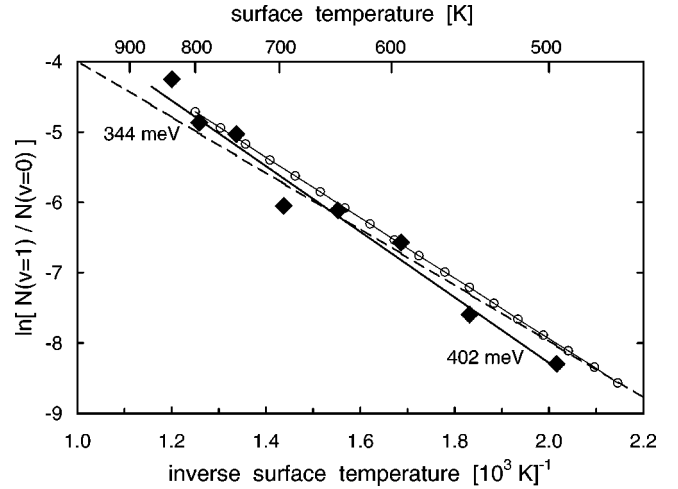


FIG. 6. Arrhenius plot of the relative population in the state $v''=1$ as a function of the inverse surface temperature T_S^{-1} . The straight line is a least-squares fit to the data, the dashed line a fit with a forced equilibrium population at $T_S=\infty$, and the open symbols denote theoretical results.

Pd(100) surface thus a reduction of the activation energy occurs. Earlier an activation energy for vibrational excitation of $E=210$ meV was found for D_2 desorption from Pd(100).³⁹ Again the comparison of the heights of only two lines instead of the whole vibrational population as in the present study may be the reason for this difference.

IV. CONCLUSION

We have presented experimental results for the state-resolved desorption probability for D_2 from Pd(100). The experimental findings, the rotational cooling and vibrational heating of molecules desorbing from the clean surface, can be explained by a quantum dynamic calculation based on a six-dimensional potential-energy surface of the system hydrogen/Pd(100). The rotational energy of the desorbing molecules for the investigated vibrational ground state is lower than expected for molecules in thermal equilibrium with a Pd crystal surface. It is not possible to fit the data with a linear Boltzmann distribution, but the low- J states are more populated than expected for the equilibrium distribution. This rotational cooling can be explained via the principle of detailed balance by the rotational hindering in adsorption due to the anisotropy of the underlying potential-energy surface. The vibrational temperature in desorption, on the other hand, is larger than expected for thermal equilibrium with the surface temperature. This vibrational heating is mainly caused by adiabatic effects due to the lowering of the vibrational frequency upon dissociation.

¹K. Christmann, Surf. Sci. Rep. **9**, 1 (1988).

²A. Groß, Surf. Sci. Rep. **32**, 291 (1998).

³G.-J. Kroes, Prog. Surf. Sci. **60**, 1 (1999).

⁴S. Wilke and M. Scheffler, Phys. Rev. B **53**, 4926 (1996).

⁵S. Wilke and M.H. Cohen, Surf. Sci. **380**, L446 (1997).

⁶A. Eichler, G. Kresse, and H. Hafner, Surf. Sci. **397**, 116 (1998).

⁷V. Ledentu, W. Dong, and P. Sautet, Surf. Sci. **412/413**, 518 (1998).

- ⁸B. Hammer, M. Scheffler, K.J. Jacobsen, and J.K. Nørskov, Phys. Rev. Lett. **73**, 1400 (1994).
- ⁹J.A. White, D.M. Bird, M.C. Payne, and I. Stich, Phys. Rev. Lett. **73**, 1404 (1994).
- ¹⁰G. Wiesenekker, G.J. Kroes, and E.J. Baerends, J. Chem. Phys. **104**, 7344 (1996).
- ¹¹R.A. Olsen, G.J. Kroes, and E.J. Baerends, J. Chem. Phys. **111**, 11 155 (1999).
- ¹²A. Groß, S. Wilke, and M. Scheffler, Phys. Rev. Lett. **75**, 2718 (1995).
- ¹³A. Groß and M. Scheffler, Phys. Rev. B **57**, 2493 (1998).
- ¹⁴A. Eichler, J. Hafner, A. Groß, and M. Scheffler, Phys. Rev. B **59**, 13 297 (1999).
- ¹⁵A. Eichler, J. Hafner, A. Groß, and M. Scheffler, Chem. Phys. Lett. **311**, 1 (1999).
- ¹⁶A. Groß, C.M. Wei, and M. Scheffler, Surf. Sci. **416**, L1095 (1998).
- ¹⁷A. Groß and M. Scheffler, Phys. Rev. B **61**, 8425 (2000).
- ¹⁸G.J. Kroes, E.J. Baerends, and R.C. Mowrey, J. Chem. Phys. **107**, 3309 (1997).
- ¹⁹D.A. McCormack, G.J. Kroes, R.A. Olsen, E.J. Baerends, and R.C. Mowrey, J. Chem. Phys. **110**, 7008 (1999).
- ²⁰J. Dai and J.C. Light, J. Chem. Phys. **107**, 1676 (1997).
- ²¹J. Dai and J.C. Light, J. Chem. Phys. **108**, 7816 (1998).
- ²²R.A. Olsen, G.J. Kroes, O.M. Løvvik, and E.J. Baerends, J. Chem. Phys. **107**, 10 652 (1997).
- ²³K.D. Rendulic, G. Anger, and A. Winkler, Surf. Sci. **208**, 404 (1989).
- ²⁴K.D. Rendulic and A. Winkler, Surf. Sci. **299/300**, 261 (1994).
- ²⁵M. Gostein and G.O. Sitz, J. Chem. Phys. **106**, 7378 (1997).
- ²⁶G. Comsa, R. David, and B.-J. Schumacher, Surf. Sci. **95**, L210 (1980).
- ²⁷C.T. Rettner, D.J. Auerbach, C. Tully, and A.W. Kleyn, J. Chem. Phys. **100**, 13 021 (1996).
- ²⁸L. Schröter, S. Küchenhoff, R. David, W. Brenig, and H. Zacharias, Surf. Sci. **261**, 243 (1992).
- ²⁹D. Wetzig, M. Rutkowski, and H. Zacharias, Phys. Status Solidi A **159**, 263 (1997).
- ³⁰B.E. Hayden and C.L.A. Lamont, Phys. Rev. Lett. **63**, 1823 (1989).
- ³¹G. Anger, A. Winkler, and K.D. Rendulic, Surf. Sci. **220**, 1 (1989).
- ³²H.F. Berger and K.D. Rendulic, Surf. Sci. **253**, 325 (1991).
- ³³C.T. Rettner, D.J. Auerbach, and H.A. Michelsen, Phys. Rev. Lett. **68**, 1164 (1992).
- ³⁴H.A. Michelsen, C.T. Rettner, and D.z. Auerbach, Surf. Sci. **272**, 65 (1992).
- ³⁵C.T. Rettner, H.A. Michelsen, and D.J. Auerbach, J. Chem. Phys. **102**, 4625 (1996).
- ³⁶E. Watts and G.O. Sitz, J. Chem. Phys. **111**, 9791 (1999).
- ³⁷L. Schröter, Chr. Trame, R. David, and H. Zacharias, Surf. Sci. **272**, 229 (1992).
- ³⁸L. Schröter, R. David, and H. Zacharias, Surf. Sci. **258**, 259 (1991).
- ³⁹L. Schröter, H. Zacharias, and R. David, Phys. Rev. Lett. **62**, 571 (1989).
- ⁴⁰A. Groß and M. Scheffler, Chem. Phys. Lett. **256**, 417 (1996).
- ⁴¹G. Comsa, R. David, and B.J. Schumacher, Surf. Sci. **85**, 45 (1979).
- ⁴²E. Fromm and E. Gebhard, *Gase und Kohlenstoffe in Metallen* (Springer, Berlin, 1976).
- ⁴³G. Hilber, A. Lago, and R. Wallenstein, J. Opt. Soc. Am. B **4**, 1753 (1987).
- ⁴⁴W. Meier, H. Rottke, H. Zacharias, and K.H. Welge, J. Chem. Phys. **83**, 4360 (1985).
- ⁴⁵W. Meier, H. Rottke, and H. Zacharias, Inst. Phys. Conf. Ser. **94**, 93 (1988).
- ⁴⁶W. Brenig, T. Brunner, A. Groß, and R. Russ, Z. Phys. B: Condens. Matter **93**, 91 (1993).
- ⁴⁷D. Wetzig, R. Dopheide, M. Rutkowski, R. David, and H. Zacharias, Phys. Rev. Lett. **76**, 463 (1996).
- ⁴⁸C.H. Greene and R.N. Zare, J. Chem. Phys. **78**, 6741 (1983).
- ⁴⁹D. Wetzig, M. Rutkowski, W. Etereich, R. David, and H. Zacharias, Surf. Sci. **402**, 232 (1998).
- ⁵⁰M. Beutl, M. Riedler, and K.D. Rendulic, Chem. Phys. Lett. **247**, 249 (1995).
- ⁵¹A. Groß, S. Wilke, and M. Scheffler, Surf. Sci. **357**, 614 (1996).
- ⁵²M. Beutl, M. Riedler, and K.D. Rendulic, Chem. Phys. Lett. **256**, 33 (1996).
- ⁵³G.R. Darling and S. Holloway, Rep. Prog. Phys. **58**, 1595 (1995).
- ⁵⁴A. Groß and M. Scheffler, Prog. Surf. Sci. **53**, 187 (1996).